Knots and Non-Hermitian Bloch Bands

Haiping Hu[1,2] and Erhai Zhao[1,*]

[1]*Department of Physics and Astronomy, George Mason University, Fairfax, Virginia 22030, USA*
[2]*Department of Physics and Astronomy, University of Pittsburgh, Pittsburgh, Pennsylvania 15260, USA*

Knots have a twisted history in quantum physics. They were abandoned as failed models of atoms. Only much later was the connection between knot invariants and Wilson loops in topological quantum field theory discovered. Here we show that knots tied by the eigenenergy strings provide a complete topological classification of one-dimensional non-Hermitian (NH) Hamiltonians with separable bands. A $\mathbb{Z}_2$ knot invariant, the global biorthogonal Berry phase Q as the sum of the Wilson loop eigenphases, is proved to be equal to the permutation parity of the NH bands. We show the transition between two phases characterized by distinct knots occur through exceptional points and come in two types. We further develop an algorithm to construct the corresponding tight-binding NH Hamiltonian for any desired knot, and propose a scheme to probe the knot structure via quantum quench. The theory and algorithm are demonstrated by model Hamiltonians that feature, for example, the Hopf link, the trefoil knot, the figure-8 knot, and the Whitehead link.

Extending topological band theory to non-Hermitian (NH) systems has significantly broadened and deepened our understanding about the topology of Bloch bands. NH Hamiltonians [1–9] are effective descriptions of a diverse set of many-body systems ranging from photonic systems with gain or loss [10–31] to quasiparticles of finite lifetime [32–39]. In contrast to Hermitian systems, NH Hamiltonians have complex eigenenergies. This unique property gives rise to a number of intricate phenomena without Hermitian counterparts including, for example, the exceptional point (EP), where eigenstates coalesce [40–46], and the NH skin effect [47–62], where an extensive number of eigenmodes are localized at the boundary. A synopsis of earlier NH band theory is the classification of topologically distinct NH Hamiltonians based on symmetry [63–68] akin to the Hermitian tenfold way [69–72]. This classification scheme starts by distinguishing two types of band gaps, the line gap and point gap. While NH bands with line gaps can be continuously deformed to their Hermitian counterparts, the point-gap topology is intrinsically NH [73–75] and explains the NH skin effect.

Recently it was recognized that the NH band theory in Refs. [63–66] based on the gap dichotomy is incomplete. A NH Hamiltonian may not possess a well-defined point or line gap. A more general theory only assumes separable bands [76], i.e., the eigenenergies $E_j(\boldsymbol{k}) \neq E_l(\boldsymbol{k})$ for all $j \neq l$ and crystal momentum $\boldsymbol{k}$. Moreover the ubiquitous twisting and braiding of complex eigenenergies give rise to new topological invariants. For example, in one dimension, as k is varied form 0 to 2π, the eigenenergy trajectories $\{E_j(k)\}$ may form a "braid" (see Fig. 1 below). Two topologically distinct NH band structures (two braids)

cannot be continuously deformed into each other while keeping the bands separable. Based on homotopy analysis, recent work established that the distinct topological sectors of 1D NH Hamiltonians with N separable bands correspond to the conjugacy classes of the braid group B_N [77,78]. Unfortunately, homotopy theory alone does not offer an algorithm to compute the invariants directly from the Hamiltonian [79]. This raises the following open questions. (i) Given a generic NH Hamiltonian, how to

	Hopf link	trefoil knot	figure-8 knot	Whitehead link
Braid word	τ_1^2	τ_1^3	$\tau_1\tau_2^{-1}\tau_1\tau_2^{-1}$	$\tau_1\tau_2^{-1}\tau_1\tau_2^{-1}\tau_2^{-1}$
Braid diagram				
Knot				
Non-Hermitian band structure				
Q	0	π	0	π
Hamiltonian	T_2	T_3	H_8	H_w

FIG. 1. Four examples of links and knots in 1D NH Bloch bands. Braid operator τ_i (τ_i^{-1}) denotes the ith string crossing over (under) the $(i+1)$th string from the left. Colors label different knot components. Q is the biorthogonal Berry phase defined in Eq. (3). The four knots are realized by NH Hamiltonians T_2, T_3 as defined in Eq. (6), H_8 and H_w [81], respectively. The eigenenergy strings are shown in space (ReE, ImE, k).

determine its topological invariant? (ii) How to describe the phase transition between two topologically distinct phases? (iii) How to design a NH Hamiltonian whose bands form a desired braid pattern?

In this Letter, we answer these questions by developing a knot theory for NH Hamiltonians. We prove that the topology of 1D NH Hamiltonians with separable bands is fully characterized by the knots (or links) formed by the eigenenergy strings, and the topological invariants are thus knot invariants. This perspective based on knots enables us to predict two types of phase transitions accompanied by the emergence of EPs and abrupt changes in the biorthogonal Wannier centers. We also present an algorithm to design tight-binding Hamiltonians to realize arbitrary knots, and demonstrate how the knots could be revealed from quantum quench experiments and realized in electric circuits and photonic arrays. In contrast to the various knots residing in the 3D k space and formed by the zero-energy nodal lines of topological semimetals [86–99], the knots here live in the energy-momentum space and describe the topology of the entire NH band structures.

Knot classification of non-Hermitian band structures.— Our first main result is that 1D NH Hamiltonians with separable bands and no symmetry are completely classified by knots inside a solid torus. It follows that a topological invariant of the band structure must be a knot invariant. To prove this statement, first we summarize the results of Refs. [77,78]. A 1D NH band structure with N separable bands defines a map from the Brillouin zone, a circle S^1, to the configuration space $X_N = (\text{Conf}_N \times F_N)/S_N$. Here Conf_N is the ordered N tuples of complex energy eigenvalues, the quotient space $F_N = U(N)/U^N(1)$ describes the energy eigenvectors, and S_N is the permutation group. Since $\pi_1(F_N) = 0$, the equivalent classes of non-based map $[S^1, X_N]$ can be reduced to $[S^1, \text{Conf}_N/S_N]$, and further to the conjugacy classes of the braid group $B_N = \pi_1(\text{Conf}_N/S_N)$ [77,78]. While this formal result based on homotopy theory is rigorous, the conjugacy classes of B_N are hard to compute or visualize [80]. Here, we further relate them to knots. Notice that the braids of energy eigenvalues (constructed explicitly below) are *closed* due to the periodicity of the Brillouin zone, so the braid space is a solid torus. A theorem in knot theory dictates that two closed N braids in B_N can be smoothly deformed into each other in the solid torus iff they are conjugate to each other [80]. Thus, thanks to the one-to-one correspondence between the conjugacy class of N braids and knots, we reach the conclusion that knots provide a natural language to classify 1D NH Bloch bands.

It is physically intuitive to construct the knot for a given 1D NH Hamiltonian $H(k)$. The procedure is outlined as follows. The complex eigenenergies form a set $\mathcal{E} = \{E_j(k)\}$ with band index $j = 1, \ldots, N$. They are the roots of the characteristic polynomial (ChP)

$$f(\lambda, k) = \det[\lambda - H(k)] = \prod_{j=1}^{N} [\lambda - E_j(k)]. \quad (1)$$

As k evolves from 0 to 2π, the trajectory of $E_i(k)$ defines a *string* in the 3D space spanned by $(\text{Re}E, \text{Im}E, k)$. Overall N such strings may tangle with each to form a braid shown in Fig. 1. A braid can be faithfully described by its braid diagram obtained by projecting the N strings onto a chosen 2D plane parallel to the vertical k axis. A braid diagram consists of a sequence of string crossings, each characterized by a *braid operator* τ_i in Artin's notation. For instance, when projected on plane $\text{Im}E = +\infty$, τ_i (τ_i^{-1}) is defined by $\text{Re}E_i = \text{Re}E_{i+1}$ and $\text{Im}E_i < \text{Im}E_{i+1}(\text{Im}E_i > \text{Im}E_{i+1})$. In other words, τ_i (τ_i^{-1}) indicates that the ith string crosses over (under) the $(i + 1)$th string from the left. Note that two nonadjacent braid operators commute: $\tau_i\tau_j = \tau_j\tau_i$ for $|j - i| \geq 2$, and $\tau_i\tau_{i+1}\tau_i = \tau_{i+1}\tau_i\tau_{i+1}$. The entire braid is then specified by its braid word, a product of braid operators, see Fig. 1. The set $\mathcal{E}$ is identical for $k = 0$ and $k = 2\pi$, so the braid is closed and becomes a knot (oriented with increasing k) in the $(\text{Re}E, \text{Im}E, k)$ space, which is topologically a solid torus. The end result of k evolution over one period 2π is the permutation

$$\sigma = \begin{pmatrix} E_1(0) & E_2(0) & \ldots & E_N(0) \\ E_1(2\pi) & E_2(2\pi) & \ldots & E_N(2\pi) \end{pmatrix}. \quad (2)$$

As usual, we define its parity $P(\sigma) = \pm 1$ if σ can be expressed as an even or odd number of transpositions.

The braid diagram may not be unique for a given band structure. Different choices of the projection plane yield isotopic braids related to each other by Reidemeister moves. Moreover, choosing different starting points k_0 for the k interval $[k_0, k_0 + 2\pi]$ corresponds to braids within the same conjugacy class. This provides a clear understanding of why the conjugacy classes, not the elements, of B_N are used for classification. These different choices, however, always yield the same unique knot, which is invariant under Reidemeister moves or translations along the k axis. Thus using knots to describe the NH band structure is not only natural but also economical, free from the arbitrariness in braid representations. Topologically distinct NH band structures correspond to distinct knots. Figure 1 lists four knots, known as the Hopf link, trefoil knot, figure-8 knot, and Whitehead link. The associated braids are also shown. To avoid clutter, hereafter we will also refer to links loosely as knots.

Knot invariants.—It follows immediately that 1D NH bands are characterized by knot invariants [100,101]. In addition to the well-known polynomial invariants [81], here we introduce a $\mathbb{Z}_2$ topological invariant Q and relate it to the parity of band permutations defined earlier. For NH Hamiltonians, the right and left eigenvectors are defined as $H(k)|\psi_n\rangle = E_n(k)|\psi_n\rangle$ and $H^\dagger(k)|\chi_n\rangle = E_n^*(k)|\chi_n\rangle$, which

satisfy the biorthogonal normalization $\langle \chi_m | \psi_n \rangle = \delta_{mn}$ [102]. Define the non-Abelian Berry connection $A_B^{mn} = i \langle \chi_m | \partial_k | \psi_n \rangle$ and the global biorthogonal Berry phase [103]

$$Q = \oint_0^{2\pi} dk \, \text{Tr}[A_B]. \quad (3)$$

One can prove [81] that Q is quantized to 0 (π) when the band permutation σ is even (odd),

$$e^{iQ} = (-1)^{P(\sigma)}. \quad (4)$$

While Q is indeed a knot invariant, due to its $\mathbb{Z}_2$ nature it only coarsely classifies knots into two groups. For example, the Hopf and figure-8 knot have the same $Q = 0$, and similarly trefoil and Whitehead knot have $Q = \pi$. In Hermitian systems, Wilson loop provides a powerful characterization of band topology [104–106]. For NH systems, we define the biorthogonal Wilson loop from the Berry connection

$$W_B = \mathcal{P} e^{i \oint_0^{2\pi} dk A_B}, \quad (5)$$

where P denotes path ordering. Its eigenphases ν_n, defined by $W_B | \mu_n \rangle = e^{i\nu_n} | \mu_n \rangle$, are the Wannier centers [31,107,108]. It can be shown [81] that $Q = \sum_n \nu_n$.

A toy model: The twister Hamiltonian.—To illustrate different knots and their phase transitions, we introduce a simple two-band NH Hamiltonian

$$T_n = \begin{pmatrix} 0 & e^{ink} \\ 1 & 0 \end{pmatrix}, \quad (6)$$

where n counts the number of twists of the two band strings, $E_\pm = \pm e^{i(nk/2)}$, as k evolves from 0 to 2π. The braid word of T_n is simply τ_1^n. The twister [109] Hamiltonian T_n for $n = 0, 1, 2$ gives rise to the unlink, unknot, and Hopf link, respectively. We will use T_n as a building block to construct a model with two tunable parameters (m_1, m_2),

$$H_{12}(k) = im_1 \sigma_z + m_2 T_1 + T_2. \quad (7)$$

It has three topologically distinct phases, the Hopf link (blue region), the unlink (green), and the unknot (pink) phase; see the phase diagram in Fig. 2(b). The phase boundaries are given by $m_1^2 + m_2^2 = 1$ and $m_2 = \pm m_1 - 1$. The knot topology is apparent from the two eigenenergy strings (blue and red solid lines in insets). For the unlink, the two strings do not braid, each forming a loop; for the Hopf link, the two strings braid twice, and the two loops are linked; for the unknot, the two strings braid once to form one single loop. We emphasize that all three phases here exhibit NH skin effect [47–52,54–62] because projecting the knot onto the complex E plane yields a band structure
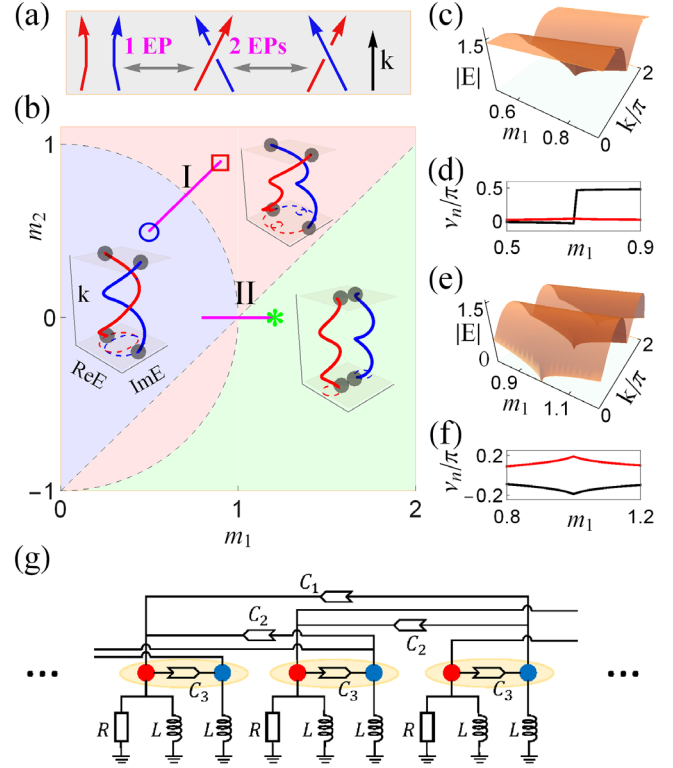

FIG. 2. Phase diagram and phase transitions of $H_{12}(k)$ defined in Eq. (7). (a) Schematic of knot transitions. Type-I (type-II) transition occurs by going through one (two) EP. (b) The phase diagram of H_{12} with parameters m_1 and m_2. The blue, pink, and green regions label the Hopf link (τ_1^2), unknot (τ_1), and unlink phase (τ_1^0), respectively. In each region, a representative band structure is plotted. (c) and (e) Eigenenergy $|E(m_1, k)|$ along the cut labeled by I and II, respectively, in (b): an EP is visible at $(1/\sqrt{2}, \pi)$ in (c), while there are two EPs at $(1,0)$ and $(1, \pi)$ in (e). (d) and (f) The Wannier centers ν_n along the cut I and II. (g) Schematic of a periodic electric circuit that realizes H_{12}. The unit cell (oval) contains two "sites," the red and blue nodes, connected by resistors R, inductors L, and negative impedance converters $C_{1,2,3}$; see Supplemental Material [81] for details.

(dash lines) with a point gap [73–75]. Previous classification framework [63–68] based on line or point gaps however cannot distinguish these phases or describe their phase transitions. The classification presented here based on knots is finer and complete.

Phase transition through exceptional points.—A transition between two phases characterized by different knots must occur through the crossing of the strings, i.e., through band degeneracy points. There are two kinds of band degeneracies in NH systems, the exceptional point (EP) or nondefective degeneracy point (NDP). The key difference is that EPs are defective, where the eigenvectors coalesce, leaving the Hamiltonian non-diagonalizable, while at an NDP, the eigenstates remain distinct. For a general 1D NH band with no symmetry, NDPs are unstable and will split into several EPs by small perturbations [110]. The proof of this statement and an example can be found in the

Supplemental Material [81]. Thus we are led to the conclusion that a transition between phases of distinct knots is accompanied by exceptional points.

There are two scenarios for two strings to undergo a "knot transition" and they are sketched in Fig. 2(a). In a type-I transition, two strings change from cross to no-cross (or vice versa) by going through an EP; the braid word $\tau_i^{\pm 1} \to \tau_i^0$ and Q also changes. One example is trefoil knot transforming to Hopf link via $\tau_1 \to \tau_1^0$. A type-II transition occurs when an overcross becomes an undercross or vice versa, so the braid word $\tau_i \to \tau_i^{-1}$. It is usually accompanied by two EPs, while Q remains the same. For $H_{12}(k)$, the transition from the Hopf link to the unknot along the line $m_1 = m_2$ belongs to type I and the EP is located at $(m_1, k) = (1/\sqrt{2}, \pi)$, as shown in Fig. 2(c). The transition from the Hopf link to the unlink along the $m_2 = 0$ line is of type II, with two EPs located at $(m_1, k) = (1, 0)$ and $(1, \pi)$ as shown in Fig. 2(d). Note that the Wannier centers undergo abrupt changes at these transitions, see Figs. 2(d) and 2(f).

How to design knotty Hamiltonians.—Beyond these simple knots, it becomes challenging to construct the tight-binding Hamiltonian $H_K(k)$ whose bands tie into certain given knot K. Here we outline a solution to this problem, which aids the experimental realization and probe of NH knots. The key is to find a ChP $f(\lambda, k)$ with $\lambda \in \mathbb{C}$ and $k \in [0, 2\pi]$ whose roots produce the desired eigenenergy strings. Our algorithm consists of two steps [81]. In the first step, $f(\lambda, k)$ is constructed from the data of knot K. From the braid diagram of K, decompose the permutation σ into a series of cycles $\sigma = s_1 s_2 \dots$ with l_n the length of cycle s_n. For each cycle, standard trigonometrical parametrization [81,111] generates two real functions $F_n(k)$, $G_n(k)$. The strings in cycle s_n are given by coordinates $[F_n(k_n^j), G_n(k_n^j), k]$ with $k_n^j = (k + 2\pi j_n)/l_n$ and $j_n = 0, \dots, l_n - 1$. Thus the roots of the following ChP,

$$f(\lambda, k) = \prod_{s_n} \prod_{j_n} [\lambda - F_n(k_n^j) - iG_n(k_n^j)], \tag{8}$$

yield the desired knot K. The ChP obtained is a power series of λ, $f(\lambda, k) = \lambda^N + \sum_{j=0}^{N-1} \zeta_j(k) \lambda^j$, where $\zeta_j(k)$ is a Laurent series of $e^{\pm ik}$. In the second step, Hamiltonian H_K is constructed from $f(\lambda, k)$ above: it is a sparse matrix [81] with the only nonzero elements being

$$H_K^{i+1,i} = 1, \quad i = 1, 2, \dots, N - 1;$$
$$H_K^{i,1} = -\zeta_{N-i}(k), \quad i = 1, 2, \dots, N. \tag{9}$$

For example, applying this algorithm to braid word τ_1^n yields the twister Hamiltonian T_n. The NH Hamiltonians for the figure-8 knot and Whitehead link, H_8 and H_w shown in Fig. 1, are similarly obtained. Their explicit expressions are lengthy and can be found in the Supplemental Material

[81]. In general, more complicated knots require longer-range couplings in the tight-binding Hamiltonian.

Experimental realization and probe of knots.—The various proposed knots and their associated NH Hamiltonians can be realized in platforms such as photonic lattices or electric circuits [112]. For the former, the asymmetric coupling between the sites (ring resonators) can be implemented via auxiliary microring cavities, see Ref. [81] for details. For the latter, the NH Hamiltonians can be simulated by the admittance matrix. For example, the twister Hamiltonian H_{12} is simulated by the periodic circuit shown in Fig. 2(g). It consists of resistors R, inductors L, and negative impedance converters C_i that provide intra- and interunit cell couplings, for details see Ref. [81]. Measurement of the admittance spectrum [60,62,113] yields $\{E_j(k)\}$, which provides a direct probe of the knotted band structures and the EPs.

An alternative probe of knots is through the eigenstates. As an example, consider the two-band system $H_{12}(k)$ where the eigenstates can be accessed via Bloch state tomography [114–118]. Each of the two right eigenstates $|\psi_{1,2}(k)\rangle$ corresponds to a point on the Bloch sphere. As k is varied, their trajectories trace out two curves (in red and blue) on the Bloch sphere as illustrated in Fig. 3. For the Hopf-link phase (a), each curve is a closed loop, and they intersect twice. In the unlink phase (c), we have two closed loops that remain separated. Both phases have even permutation parity, $Q = 0$. In contrast, in the unknot phase (b), the red curve joins the blue curve to form a single loop, and $Q = \pi$. It is clear from this example that the knot topology of two eigenenergy strings translates to characteristic crossing patterns of the eigenvector loops on the Bloch sphere, which can be distinguished from Bloch state tomography. The invariant Q can also be read out directly.

We propose an effective way to prepare $|\psi_{1,2}(k)\rangle$ via quantum quench. From an (arbitrary) initial state $|\xi_0\rangle$ at time $t = 0$, the system evolves according to $H_{12}(k)$. Let the jth eigenenergy $E_j(k) = \epsilon_j - i\gamma_j$; the state at later time t is $|\xi(k,t)\rangle = \sum_j e^{-i\epsilon_j t} e^{-\gamma_j t} \langle \chi_j | \xi_0 \rangle |\psi_j\rangle$ with $\hbar = 1$. Thus,
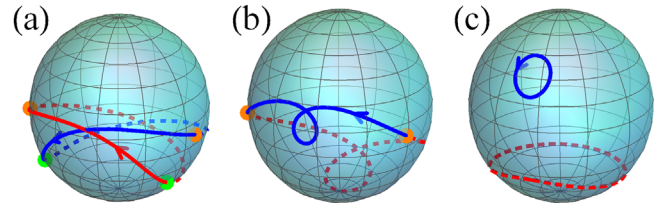

FIG. 3. Signatures of knots after quantum quench. The red and blue curves are the eigenvectors $|\psi_{1,2}(k)\rangle$ of $H_{12}(k)$ on the Bloch sphere. From an initial state $|\xi_0\rangle = (1, 0)^T$ (north pole), the state evolves with $H_{12}(k)$ and after a long time falls into the solid line part of the eigenstates. The arrow denotes increasing k from 0 to 2π, and the orange (green) dots represent the $k = 0$ ($k = \pi$) mode. The parameters are (a) $m_1 = m_2 = 0.5$, the Hopf-link phase; (b) $m_1 = m_2 = 0.9$, the unknot phase; and (c) $m_1 = 1.2, m_2 = 0$, the unlink phase.

after a long time, the time-evolved state will be purified and fall into the eigenstate with smaller γ_j. Our numerical simulation of the quench dynamics verifies that starting from $|\xi_0\rangle = (1, 0)^T$ (the north pole), long-time evolution will bring the state to the solid curves in Fig. 3 (the dashed curves are reached by evolution with $-H_{12}$). While the k-resolved tomography measurement of the quenched state does not yield the full band structure, different knots can be distinguished by their signatures in the eigenvectors as shown in Fig. 3 [81].

Going beyond conjugacy classes of braid groups, we have established a knot classification of generic 1D NH Hamiltonians with separable bands: topologically distinct NH bands are described by different knots, and their transitions are through EPs. A simple model is built from T_n to showcase various knots, and an algorithm is presented to construct the corresponding tight-binding Hamiltonian for any given knot. We have demonstrated how these knots can be experimentally realized and probed. Other physical consequences of the knotted bands, including the relation between the NH knots and skin effect, will be left for further study [81]. An important open problem is to extend the analysis to higher dimensions and other symmetry classes, where the interplay of band braiding, eigenstate topology, and symmetries gives rise to rich unexplored phenomena, e.g., torsion invariants [77,78].

---

*ezhao2@gmu.edu
[1] C. M. Bender, Making sense of non-Hermitian Hamiltonians, Rep. Prog. Phys. 70, 947 (2007).
[2] I. Rotter, A non-Hermitian Hamilton operator and the physics of open quantum systems, J. Phys. A 42, 153001 (2009).
[3] V. M. Martinez Alvarez, J. E. Barrios Vargas, M. Berdakin, and L. E. F. Foa Torres, Topological states of non-Hermitian systems, Eur. Phys. J. Special Topics 227, 1295 (2018).
[4] R. El-Ganainy, K. G. Makris, M. Khajavikhan, Z. H. Musslimani, S. Rotter, and D. N. Christodoulides, Non-Hermitian physics and PT symmetry, Nat. Phys. 14, 11 (2018).
[5] E. J. Bergholtz, J. C. Budich, and F. K. Kunst, Exceptional topology of non-Hermitian systems, arXiv:1912.10048.
[6] N. Moiseyev, Non-Hermitian Quantum Mechanics (Cambridge University Press, New York, 2011).
[7] A. Ghatak and T. Das, New topological invariants in non-Hermitian systems, J. Phys. Condens. Matter 31, 263001 (2019).
[8] L. E. F. Foa Torres, Perspective on topological states of non-Hermitian systems, J. Phys. Mater. 3, 014002 (2019).
[9] Y. Ashida, Z. Gong, and Masahito Ueda, Non-Hermitian physics, arXiv:2006.01837.
[10] K. G. Makris, R. El-Ganainy, D. N. Christodoulides, and Z. H. Musslimani, Beam Dynamics in $\mathcal{PT}$ Symmetric Optical Lattices, Phys. Rev. Lett. 100, 103904 (2008).
[11] A. Regensburger, C. Bersch, M.-A. Miri, G. Onishchukov, D. N. Christodoulides, and U. Peschel, Parity-time synthetic photonic lattices, Nature (London) 488, 167 (2012).
[12] B. Peng, . K. Özdemir, S. Rotter, H. Yilmaz, M. Liertzer, F. Monifi, C. M. Bender, F. Nori, and L. Yang, Loss-induced suppression and revival of lasing, Science 346, 328 (2014).
[13] H. Jing, S. K. Özdemir, X.-Y. Lü, J. Zhang, L. Yang, and F. Nori, $\mathcal{PT}$-Symmetric Phonon Laser, Phys. Rev. Lett. 113, 053604 (2014).
[14] L. Feng, Z. J. Wong, R.-M. Ma, Y. Wang, and X. Zhang, Single-mode laser by parity-time symmetry breaking, Science 346, 972 (2014).
[15] S. Malzard, C. Poli, and H. Schomerus, Topologically Protected Defect States in Open Photonic Systems with Non-Hermitian Charge-Conjugation and Parity-Time Symmetry, Phys. Rev. Lett. 115, 200402 (2015).
[16] J. M. Zeuner, M. C. Rechtsman, Y. Plotnik, Y. Lumer, S. Nolte, M. S. Rudner, M. Segev, and A. Szameit, Observation of a Topological Transition in the Bulk of a non-Hermitian System, Phys. Rev. Lett. 115, 040402 (2015).
[17] B. Zhen, C. W. Hsu, Y. Igarashi, L. Lu, I. Kaminer, A. Pick, S.-L. Chua, J. D. Joannopoulos, and M. Soljačić, Spawning rings of exceptional points out of Dirac cones, Nature (London) 525, 354 (2015).
[18] C. Poli, M. Bellec, U. Kuhl, F. Mortessagne, and H. Schomerus, Selective enhancement of topologically induced interface states in a dielectric resonator chain, Nat. Commun. 6, 6710 (2015).
[19] S. Weimann, M. Kremer, Y. Plotnik, Y. Lumer, S. Nolte, K. G. Makris, M. Segev, M. C. Rechtsman, and A. Szameit, Topologically protected bound states in photonic paritytime-symmetric crystals, Nat. Mater. 16, 433 (2017).
[20] P. St-Jean, V. Goblot, E. Galopin, A. Lematre, T. Ozawa, L. Le Gratiet, I. Sagnes, J. Bloch, and A. Amo, Lasing in topological edge states of a one-dimensional lattice, Nat. Photonics 11, 651 (2017).
[21] L. Xiao et al., Observation of topological edge states in parity-time-symmetric quantum walks, Nat. Phys. 13, 1117 (2017).
[22] X. Zhan, L. Xiao, Z. Bian, K. Wang, X. Qiu, B. C. Sanders, W. Yi, and P. Xue, Detecting Topological Invariants in Nonunitary Discrete-Time Quantum Walks, Phys. Rev. Lett. 119, 130501 (2017).
[23] H. Zhao, P. Miao, M. H. Teimourpour, S. Malzard, R. El-Ganainy, H. Schomerus, and L. Feng, Topological hybrid silicon microlasers, Nat. Commun. 9, 981 (2018).
[24] M. Parto, S. Wittek, H. Hodaei, G. Harari, M. A. Bandres, J. Ren, M. C. Rechtsman, M. Segev, D. N. Christodoulides, and M. Khajavikhan, Edge-Mode Lasing in 1D Topological Active Arrays, Phys. Rev. Lett. 120, 113901 (2018).
[25] J. Zhang, B. Peng, . K. zdemir, K. Pichler, D. O. Krimer, G. Zhao, F. Nori, Y.-x. Liu, S. Rotter, and L. Yang, A phonon laser operating at an exceptional point, Nat. Photonics 12, 479 (2018).
[26] M. A. Bandres, S. Wittek, G. Harari, M. Parto, J. Ren, M. Segev, D. N. Christodoulides, and M. Khajavikhan, Topo-

logical insulator laser: Experiments, Science **359,** eaar4005 (2018).

[27] Y. N. Joglekar and A. K. Harter, Passive parity-time-symmetry-breaking transitions without exceptional points in dissipative photonic systems, Photonics Res. **6,** A51 (2018).

[28] H. Zhou, C. Peng, Y. Yoon, C. W. Hsu, K. A. Nelson, L. Fu, J. D. Joannopoulos, M. Soljačić, and B. Zhen, Observation of bulk Fermi arc and polarization half charge from paired exceptional points, Science **359,** 1009 (2018).

[29] A. Cerjan, S. Huang, K. P. Chen, Y. D. Chong, and M. C. Rechtsman, Experimental realization of a Weyl exceptional ring, Nat. Photonics **13,** 623 (2019).

[30] J. Hou, Z. Li, Q. Gu, and C. Zhang, Non-Hermitian photonics based on charge-parity symmetry, arXiv:1904.05260.

[31] X.-W. Luo and C. Zhang, Higher-Order Topological Corner States Induced by Gain and Loss, Phys. Rev. Lett. **123,** 073601 (2019).

[32] V. Kozii and L. Fu, Non-Hermitian topological theory of finite-lifetime quasiparticles: Prediction of bulk Fermi arc due to exceptional point, arXiv:1708.05841.

[33] H. Shen and L. Fu, Quantum Oscillation from In-Gap States and Non-Hermitian Landau Level Problem, Phys. Rev. Lett. **121,** 026403 (2018).

[34] T. Yoshida, R. Peters, and N. Kawakami, Non-Hermitian perspective of the band structure in heavy-fermion systems, Phys. Rev. B **98,** 035141 (2018).

[35] Y. Xu, S.-T. Wang, and L.-M. Duan, Weyl Exceptional Rings in a Three-Dimensional Dissipative Cold Atomic Gas, Phys. Rev. Lett. **118,** 045701 (2017).

[36] M. Papaj, H. Isobe, and L. Fu, Nodal arc of disordered Dirac fermions and non-Hermitian band theory, Phys. Rev. B **99,** 201107(R) (2019).

[37] J. Li, A. K. Harter, J. Liu, L. de Melo, Y. N. Joglekar, and L. Luo, Observation of parity-time symmetry breaking transitions in a dissipative Floquet system of ultracold atoms, Nat. Commun. **10,** 855 (2019).

[38] Y. Ashida, S. Furukawa, and M. Ueda, Parity-time-symmetric quantum critical phenomena, Nat. Commun. **8,** 15791 (2017).

[39] S. Diehl, E. Rico, M. A. Baranov, and P. Zoller, Topology by dissipation in atomic quantum wires, Nat. Phys. **7,** 971 (2011).

[40] M. V. Berry, Physics of non Hermitian degeneracies, Czech. J. Phys. **54,** 1039 (2004).

[41] W D Heiss, The physics of exceptional points, J. Phys. A **45,** 444016 (2012).

[42] M.-A. Miri and A. Alù, Exceptional points in optics and photonics, Science **363,** eaar7709 (2019).

[43] K. Kawabata, T. Bessho, and M. Sato, Classification of Exceptional Points and Non-Hermitian Topological Semimetals, Phys. Rev. Lett. **123,** 066405 (2019).

[44] T. Yoshida, R. Peters, N. Kawakami, and Y. Hatsugai, Symmetry-protected exceptional rings in two-dimensional correlated systems with chiral symmetry, Phys. Rev. B **99,** 121101(R) (2019).

[45] T. Yoshida and Y. Hatsugai, Exceptional rings protected by emergent symmetry for mechanical systems, Phys. Rev. B **100,** 054109 (2019).

[46] S. Lin, L. Jin, and Z. Song, Symmetry protected topological phases characterized by isolated exceptional points, Phys. Rev. B **99,** 165148 (2019).

[47] S. Yao and Z. Wang, Edge States and Topological Invariants of Non-Hermitian Systems, Phys. Rev. Lett. **121,** 086803 (2018).

[48] F. K. Kunst, E. Edvardsson, J. C. Budich, and E. J. Bergholtz, Biorthogonal Bulk-Boundary Correspondence in Non-Hermitian Systems, Phys. Rev. Lett. **121,** 026808 (2018).

[49] S. Yao, F. Song, and Z. Wang, Non-Hermitian Chern Bands, Phys. Rev. Lett. **121,** 136802 (2018).

[50] Y. Xiong, Why does bulk boundary correspondence fail in some non-Hermitian topological models, J. Phys. Commun. **2,** 035043 (2018).

[51] T. E. Lee, Anomalous Edge State in a Non-Hermitian Lattice, Phys. Rev. Lett. **116,** 133903 (2016).

[52] K. Yokomizo and S. Murakami, Non-Bloch Band Theory of Non-Hermitian Systems, Phys. Rev. Lett. **123,** 066404 (2019).

[53] V. M. Martinez Alvarez, J. E. Barrios Vargas, and L. E. F. Foa Torres, Non-Hermitian robust edge states in one-dimension: Anomalous localization and eigenspace condensation at exceptional points, Phys. Rev. B **97,** 121401 (R) (2018).

[54] C. H. Lee and R. Thomale, Anatomy of skin modes and topology in non-Hermitian systems, Phys. Rev. B **99,** 201103(R) (2019).

[55] L. Li, C. H. Lee, S. Mu, and J. Gong, Critical non-Hermitian skin effect, Nat. Commun. **11,** 5491 (2020).

[56] C.-H. Liu, K. Zhang, Z. Yang, and S. Chen, Helical damping and anomalous critical non-Hermitian skin effect, Phys. Rev. Research **2,** 043167 (2020).

[57] Z. Yang, K. Zhang, C. Fang, and J. Hu, Auxiliary Generalized Brillouin Zone Method in Non-Hermitian Band Theory, Phys. Rev. Lett. **125,** 226402 (2020).

[58] C. H. Lee, L. Li, R. Thomale, and J. Gong, Unraveling non-Hermitian pumping: Emergent spectral singularities and anomalous responses, Phys. Rev. B **102,** 085151 (2020).

[59] A. Ghatak, M. Brandenbourger, J. van Wezel, and C. Coulais, Observation of non-Hermitian topology and its bulk-edge correspondence, Proc. Natl. Acad. Sci. U.S.A. **117,** 29561 (2020).

[60] T. Helbig, T. Hofmann, S. Imhof, M. Abdelghany, T. Kiessling, L. W. Molenkamp, C. H. Lee, A. Szameit, M. Greiter, and R. Thomale, Generalized bulkboundary correspondence in non-Hermitian topolectrical circuits, Nat. Phys. **16,** 747 (2020).

[61] L. Xiao, T. Deng, K. Wang, G. Zhu, Z. Wang, W. Yi, and P. Xue, Observation of non-hermitian bulk-boundary correspondence in quantum dynamics, Nat. Phys. **16,** 761 (2020).

[62] T. Hofmann *et al.*, Reciprocal skin effect and its realization in a topolectrical circuit, Phys. Rev. Research **2,** 023265 (2020).

[63] Z. Gong, Y. Ashida, K. Kawabata, K. Takasan, S. Higashikawa, and M. Ueda, Topological Phases of Non-Hermitian Systems, Phys. Rev. X **8,** 031079 (2018).

[64] K. Kawabata, K. Shiozaki, M. Ueda, and M. Sato, Symmetry and Topology in Non-Hermitian Physics, Phys. Rev. X **9**, 041015 (2019).

[65] H. Zhou and J. Y. Lee, Periodic table for topological bands with non-Hermitian symmetries, Phys. Rev. B **99**, 235112 (2019).

[66] C.-H. Liu and S. Chen, Topological classification of defects in non-Hermitian systems, Phys. Rev. B **100**, 144106 (2019).

[67] C.-H. Liu, H. Jiang, and S. Chen, Topological classification of non-hermitian systems with reflection symmetry, Phys. Rev. B **99**, 125103 (2019).

[68] L. Li, C. H. Lee, and J. Gong, Geometric characterization of non-Hermitian topological systems through the singularity ring in pseudospin vector space, Phys. Rev. B **100**, 075403 (2019).

[69] A. P. Schnyder, S. Ryu, A. Furusaki, and A. W. W. Ludwig, Classification of topological insulators and superconductors in three spatial dimensions, Phys. Rev. B **78**, 195125 (2008).

[70] A. Y. Kitaev, Periodic table for topological insulators and superconductors, AIP Conf. Proc. **1134**, 22 (2009).

[71] S. Ryu, A. Schnyder, A. Furusaki, and A. W. W. Ludwig, Topological insulators and superconductors: Ten-fold way and dimensional hierarchy, New J. Phys. **12**, 065010 (2010).

[72] C.-K. Chiu, J. C. Y. Teo, A. P. Schnyder, and S. Ryu, Classification of topological quantum matter with symmetries, Rev. Mod. Phys. **88**, 035005 (2016).

[73] N. Okuma, K. Kawabata, K. Shiozaki, and M. Sato, Topological Origin of Non-Hermitian Skin Effects, Phys. Rev. Lett. **124**, 086801 (2020).

[74] K. Zhang, Z. Yang, and C. Fang, Correspondence between Winding Numbers and Skin Modes in Non-Hermitian Systems, Phys. Rev. Lett. **125**, 126402 (2020).

[75] D. S. Borgnia, A. J. Kruchkov, and R.-J. Slager, Non-Hermitian Boundary Modes and Topology, Phys. Rev. Lett. **124**, 056802 (2020).

[76] H. Shen, B. Zhen, and L. Fu, Topological Band Theory for Non-Hermitian Hamiltonians, Phys. Rev. Lett. **120**, 146402 (2018).

[77] C. C. Wojcik, X.-Q. Sun, T. Bzdušek, and S. Fan, Homotopy characterization of non-Hermitian Hamiltonians, Phys. Rev. B **101**, 205417 (2020).

[78] Z. Li and R. S. K. Mong, Homotopical classification of non-Hermitian band structures, arXiv:1911.02697.

[79] Finding the conjugacy classes of B_N is hard problem, see Refs. [78,80].

[80] C. Kassel and V. Turaev, *Braid Groups* (Springer, Berlin, 2008), theorem 2.1, on page 54.

[81] See Supplemental Material at http://link.aps.org/supplemental/10.1103/PhysRevLett.126.010401 for more details on (I) the polynomial knot invariant; (II) the relation between biorthogonal Berry phase, band permutation, and Wilson loop; (III) stability of band touchings in knot transitions; (IV) the algorithm of constructing NH Hamiltonians and examples; (V) revealing knots from quench dynamics; (VI) proposal for experimental realizations of knotted Hamiltonian; (VII) NH knot and skin effect, which includes Refs. [82–85].

[82] S. Imhof *et al.*, Topolectrical-circuit realization of topological corner modes, Nat. Phys. **14**, 925 (2018).

[83] T. Helbig, T. Hofmann, C. H. Lee, R. Thomale, S. Imhof, L. W. Molenkamp, and T. Kiessling, Band structure engineering and reconstruction in electric circuit networks, Phys. Rev. B **99**, 161114(R) (2019).

[84] S. Longhi, D. Gatti, and G. D. Valle, Robust light transport in non-Hermitian photonic lattices, Sci. Rep. **5**, 13376 (2015).

[85] S. Mittal, V. V. Orre, G. Zhu, M. A. Gorlach, A. Poddubny, and M. Hafezi, Photonic quadrupole topological phases, Nat. Photonics **13**, 692 (2019).

[86] C. Zhong, Y. Chen, Z.-M. Yu, Y. Xie, H. Wang, S. A. Yang, and S. Zhang, Three-dimensional Pentagon carbon with a genesis of emergent fermions, Nat. Commun. **8**, 15641 (2017).

[87] Z. Yan, R. Bi, H. Shen, L. Lu, S.-C. Zhang, and Z. Wang, Nodal-link semimetals, Phys. Rev. B **96**, 041103(R) (2017).

[88] R. Bi, Z. Yan, L. Lu, and Z. Wang, Nodal-knot semimetals, Phys. Rev. B **96**, 201305(R) (2017).

[89] M. Ezawa, Topological semimetals carrying arbitrary Hopf numbers: Fermi surface topologies of a Hopf link, Solomon's knot, trefoil knot, and other linked nodal varieties, Phys. Rev. B **96**, 041202(R) (2017).

[90] W. Chen, H.-Z. Lu, and J.-M. Hou, Topological semimetals with a double-helix nodal link, Phys. Rev. B **96**, 041102 (R) (2017).

[91] Y. Zhou, F. Xiong, X. Wan, and J. An, Hopf-link topological nodal-loop semimetals, Phys. Rev. B **97**, 155140 (2018).

[92] L. Li, C. H. Lee, and J. Gong, Realistic Floquet Semimetal with Exotic Topological Linkages between Arbitrarily Many Nodal Loops, Phys. Rev. Lett. **121**, 036401 (2018).

[93] C. H. Lee, T. Hofmann, T. Helbig, Y. Liu, X. Zhang, M. Greiter, and R. Thomale, Imaging nodal knots in momentum space through topolectrical circuits, Nat. Commun. **11**, 4385 (2020).

[94] J. Carlström and E. J. Bergholtz, Exceptional links and twisted Fermi ribbons in non-Hermitian systems, Phys. Rev. A **98**, 042114 (2018).

[95] Johan Carlström, M. Stalhammar, J. C. Budich, and E. J. Bergholtz, Knotted non-Hermitian metals, Phys. Rev. B **99**, 161115(R) (2019).

[96] M. Stlhammar, L. Rdland, G. Arone, J. C. Budich, and E. J. Bergholtz, Hyperbolic nodal band structures and knot invariants, SciPost Phys. **7**, 019 (2019).

[97] C. H. Lee, G. Li, Y. Liu, T. Tai, R. Thomale, and X. Zhan, Tidal surface states as fingerprints of non-Hermitian nodal knot metals, arXiv:1812.02011.

[98] X. M. Yang, H. C. Wu, P. Wang, L. Jin, and Z. Song, Visualizing one-dimensional non-Hermitian topological phases, J. Phys. Commun. **4**, 095005 (2020).

[99] Z. Yang, C.-K. Chiu, C. Fang, and J. Hu, Jones Polynomial and Knot Transitions in Hermitian and Non-Hermitian Topological Semimetals, Phys. Rev. Lett. **124**, 186402 (2020).

[100] L. H. Kauffman, *Knots and Physics* (World Scientific, Singapore, 1991).

[101] V. F. R. Jones, A polynomial invariant for knots via von Neumann algebras, Bull. Am. Math. Soc. **12**, 103 (1985).

[102] D. C. Brody, Biorthogonal quantum mechanics, J. Phys. A **47**, 035305 (2014).

[103] S.-D. Liang and G.-Y. Huang, Topological invariance and global Berry phase in non-Hermitian systems, Phys. Rev. A **87**, 012118 (2013).

[104] W. A. Benalcazar, B. A. Bernevig, and T. L. Hughes, Quantized electric multipole insulators, Science **357**, 61 (2017).

[105] L. Fidkowski, T. S. Jackson, and I. Klich, Model Characterization of Gapless Edge Modes of Topological Insulators Using Intermediate Brillouin-Zone Functions, Phys. Rev. Lett. **107**, 036601 (2011).

[106] H. Hu, B. Huang, E. Zhao, and W. V. Liu, Dynamical Singularities of Floquet Higher-Order Topological Insulators, Phys. Rev. Lett. **124**, 057001 (2020).

[107] R. Yu, X. L. Qi, A. Bernevig, Z. Fang, and X. Dai, Equivalent expression of $\mathbb{Z}_2$ topological invariant for band insulators using the non-Abelian Berry connection, Phys. Rev. B **84**, 075119 (2011).

[108] J. Hou, Y.-J. Wu, and C. Zhang, Non-Hermitian topological phase transitions for quantum spin Hall insulators, arXiv:1910.14606.

[109] The name twister here refers to the phase twist, and the fact that the eigenenergy strings (see T_2, T_3 in Fig. 1) resemble a tornado or twister. It should not be confused with twistor as in twistor theory.

[110] Z. Yang, A. P. Schnyder, J. Hu, and C.-K. Chiu, Fermion doubling theorems in 2D non-Hermitian systems for Fermi points and exceptional points, arXiv:1912.02788v1.

[111] B. Bode and M. R. Dennis, Constructing a polynomial whose nodal set is any prescribed knot or link, J. Knot Theory Ramifications **28**, 1850082 (2019).

[112] E. Zhao, Topological circuits of inductors and capacitors, Ann. Phys. (Amsterdam) **399**, 289 (2018).

[113] C. H. Lee, S, Imhof, C. Berger, F, Bayer, J, Brehm, L. W. Molenkamp, T. Kiessling, and R. Thomale, Topolectrical circuits, Commun. Phys. **1**, 39 (2018).

[114] H. Hu and E. Zhao, Topological Invariants for Quantum Quench Dynamics from Unitary Evolution, Phys. Rev. Lett. **124**, 160402 (2020).

[115] P. Hauke, M. Lewenstein, and A. Eckardt, Tomography of Band Insulators from Quench Dynamics, Phys. Rev. Lett. **113**, 045303 (2014).

[116] N. Fläschner, B. S. Rem, M. Tarnowski, D. Vogel, D.-S. Lühmann, K. Sengstock, and C. Weitenberg, Experimental reconstruction of the Berry curvature in a Floquet Bloch band, Science **352**, 1091 (2016).

[117] T. Li, L. Duca, M. Reitter, F. Grusdt, E. Demler, M. Endres, M. Schleier-Smith, I. Bloch, and U. Schneider, Bloch state tomography using Wilson lines, Science **352**, 1094 (2016).

[118] E. Alba, X. Fernandez-Gonzalvo, J. Mur-Petit, J. K. Pachos, and J. J. Garcia-Ripoll, Seeing Topological Order in Time-of-Flight Measurements, Phys. Rev. Lett. **107**, 235301 (2011).